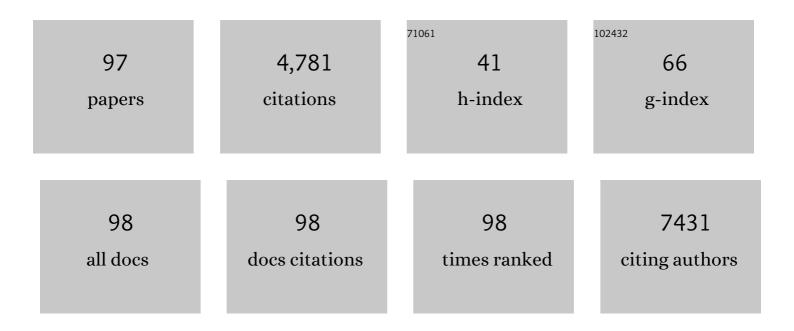
Haibing Xia

List of Publications by Year in descending order

Source: https://exaly.com/author-pdf/8264477/publications.pdf Version: 2024-02-01



#	Article	IF	CITATIONS
1	Bulk crystal growth of hybrid perovskite material CH ₃ NH ₃ PbI ₃ . CrystEngComm, 2015, 17, 665-670.	1.3	483
2	Formation of Hybrid Perovskite Tin Iodide Single Crystals by Top‧eeded Solution Growth. Angewandte Chemie - International Edition, 2016, 55, 3447-3450.	7.2	238
3	Efficient Synthesis of MCu (M = Pd, Pt, and Au) Aerogels with Accelerated Gelation Kinetics and their High Electrocatalytic Activity. Advanced Materials, 2016, 28, 8779-8783.	11.1	213
4	Synthesis of Monodisperse Quasi-Spherical Gold Nanoparticles in Water via Silver(I)-Assisted Citrate Reduction. Langmuir, 2010, 26, 3585-3589.	1.6	169
5	Novel Method for the Preparation of Polymeric Hollow Nanospheres Containing Silver Cores with Different Sizes. Chemistry of Materials, 2005, 17, 3578-3581.	3.2	152
6	Nanovoid Incorporated Ir _{<i>x</i>} Cu Metallic Aerogels for Oxygen Evolution Reaction Catalysis. ACS Energy Letters, 2018, 3, 2038-2044.	8.8	129
7	Rapid Seeded Growth of Monodisperse, Quasi-Spherical, Citrate-Stabilized Gold Nanoparticles via H ₂ O ₂ Reduction. Langmuir, 2012, 28, 13720-13726.	1.6	114
8	Fabrication of Macroscopic Freestanding Films of Metallic Nanoparticle Monolayers by Interfacial Selfâ€Assembly. Advanced Materials, 2008, 20, 4253-4256.	11.1	108
9	Simple Synthesis of Monodisperse, Quasi-spherical, Citrate-Stabilized Silver Nanocrystals in Water. Langmuir, 2013, 29, 5074-5079.	1.6	106
10	Revitalizing the Frens Method To Synthesize Uniform, Quasi-Spherical Gold Nanoparticles with Deliberately Regulated Sizes from 2 to 330 nm. Langmuir, 2016, 32, 5870-5880.	1.6	93
11	Crystallographic Investigations into Properties of Acentric Hybrid Perovskite Single Crystals NH(CH ₃) ₃ SnX ₃ (X = Cl, Br). Chemistry of Materials, 2016, 28, 6968-6974.	3.2	92
12	Facile Fabrication of AgCl@Polypyrroleâ^'Chitosan Coreâ^'Shell Nanoparticles and Polymeric Hollow Nanospheres. Langmuir, 2004, 20, 9909-9912.	1.6	85
13	Realizing a Record Photothermal Conversion Efficiency of Spiky Gold Nanoparticles in the Second Near-Infrared Window by Structure-Based Rational Design. Chemistry of Materials, 2018, 30, 2709-2718.	3.2	85
14	Intermetallic Pd ₃ Pb nanowire networks boost ethanol oxidation and oxygen reduction reactions with significantly improved methanol tolerance. Journal of Materials Chemistry A, 2017, 5, 23952-23959.	5.2	78
15	Synthesis of open-mouthed, yolk–shell Au@AgPd nanoparticles with access to interior surfaces for enhanced electrocatalysis. Chemical Science, 2015, 6, 4350-4357.	3.7	77
16	Tumor microenvironment-responsive multifunctional peptide coated ultrasmall gold nanoparticles and their application in cancer radiotherapy. Theranostics, 2020, 10, 5195-5208.	4.6	75
17	Facile Fabrication of Water-Soluble Magnetic Nanoparticles and Their Spherical Aggregates. Chemistry of Materials, 2007, 19, 4087-4091.	3.2	69
18	Top-Seeded Solution Growth, Morphology, and Properties of a Polar Crystal Cs ₂ TeMo ₃ O ₁₂ . Crystal Growth and Design, 2011, 11, 1863-1868.	1.4	69

Haibing Xia

#	Article	IF	CITATIONS
19	PdCuPt Nanocrystals with Multibranches for Enzyme-Free Glucose Detection. ACS Applied Materials & Interfaces, 2016, 8, 22196-22200.	4.0	68
20	Low Pt-content ternary PdCuPt nanodendrites: an efficient electrocatalyst for oxygen reduction reaction. Nanoscale, 2017, 9, 1279-1284.	2.8	66
21	Synthesis and Characterization of Surface-Functionalized Conducting Polyaniline-Chitosan Nanocomposite. Journal of Nanoscience and Nanotechnology, 2005, 5, 466-473.	0.9	65
22	Controlled chelation between tannic acid and Fe precursors to obtain N, S co-doped carbon with high density Fe-single atom-nanoclusters for highly efficient oxygen reduction reaction in Zn–air batteries. Journal of Materials Chemistry A, 2020, 8, 17136-17149.	5.2	64
23	A Facile Method for Synthesizing Dendritic Core–Shell Structured Ternary Metallic Aerogels and Their Enhanced Electrochemical Performances. Chemistry of Materials, 2016, 28, 7928-7934.	3.2	60
24	Synthesis of core–shell Au–Pt nanodendrites with high catalytic performance via overgrowth of platinum on in situ gold nanoparticles. Journal of Materials Chemistry A, 2015, 3, 368-376.	5.2	59
25	Effect and mechanism analysis of MnO2 on permeable reactive barrier (PRB) system for the removal of tetracycline. Chemosphere, 2018, 193, 702-710.	4.2	59
26	Synthesis of Monodisperse, Quasi-Spherical Silver Nanoparticles with Sizes Defined by the Nature of Silver Precursors. Langmuir, 2014, 30, 2498-2504.	1.6	55
27	Highly branched PtCu bimetallic alloy nanodendrites with superior electrocatalytic activities for oxygen reduction reactions. Nanoscale, 2016, 8, 5076-5081.	2.8	55
28	Size Control Synthesis of Monodisperse, Quasi-Spherical Silver Nanoparticles To Realize Surface-Enhanced Raman Scattering Uniformity and Reproducibility. ACS Applied Materials & Interfaces, 2019, 11, 17637-17646.	4.0	55
29	Ultrathin dendritic IrTe nanotubes for an efficient oxygen evolution reaction in a wide pH range. Journal of Materials Chemistry A, 2018, 6, 8855-8859.	5.2	54
30	Formation of Ordered Arrays of Oriented Polyaniline Nanoparticle Nanorods. Journal of Physical Chemistry B, 2005, 109, 12677-12684.	1.2	53
31	Kinetically Controlled Synthesis of Pt-Based One-Dimensional Hierarchically Porous Nanostructures with Large Mesopores as Highly Efficient ORR Catalysts. ACS Applied Materials & Interfaces, 2016, 8, 35213-35218.	4.0	53
32	Understanding the effect of ultrathin AuPd alloy shells of irregularly shaped Au@AuPd nanoparticles with high-index facets on enhanced performance of ethanol oxidation. Nanoscale, 2015, 7, 20105-20116.	2.8	50
33	Sizeâ€Dependent Electrostatic Chain Growth of pHâ€5ensitive Hairy Nanoparticles. Angewandte Chemie - International Edition, 2013, 52, 3726-3730.	7.2	49
34	Directed self-assembly of gold nanoparticles into plasmonic chains. Soft Matter, 2015, 11, 4562-4571.	1.2	49
35	High–Yield Production of Uniform Gold Nanoparticles with Sizes from 31 to 577 nm via Oneâ€Pot Seeded Growth and Sizeâ€Đependent SERS Property. Particle and Particle Systems Characterization, 2016, 33, 924-932.	1.2	47
36	The impact of size and surface ligand of gold nanorods on liver cancer accumulation and photothermal therapy in the second near-infrared window. Journal of Colloid and Interface Science, 2020, 565, 186-196.	5.0	47

#	Article	IF	CITATIONS
37	{331}-Faceted trisoctahedral gold nanocrystals: synthesis, superior electrocatalytic performance and highly efficient SERS activity. Nanoscale, 2015, 7, 8405-8415.	2.8	46
38	Correlation of Surface Ag Content in AgPd Shells of Ultrasmall Core–Shell Au@AgPd Nanoparticles with Enhanced Electrocatalytic Performance for Ethanol Oxidation. Journal of Physical Chemistry C, 2015, 119, 18434-18443.	1.5	45
39	Aggregation-induced emission enhancement of polycyclic aromatic alkaloid derivatives and the crucial role of excited-state proton-transfer. Chemical Communications, 2011, 47, 2907.	2.2	44
40	Kinetically controlled synthesis of AuPt bi-metallic aerogels and their enhanced electrocatalytic performances. Journal of Materials Chemistry A, 2017, 5, 19626-19631.	5.2	44
41	Freestanding monolayered nanoporous gold films with high electrocatalytic activity via interfacial self-assembly and overgrowth. Journal of Materials Chemistry A, 2013, 1, 4678.	5.2	42
42	High Yield Seedless Synthesis of High-Quality Gold Nanocrystals with Various Shapes. Langmuir, 2014, 30, 2480-2489.	1.6	42
43	Eu/Tb codoped spindle-shaped fluorinated hydroxyapatite nanoparticles for dual-color cell imaging. Nanoscale, 2016, 8, 11580-11587.	2.8	41
44	Hydrogenâ€Bondâ€Selective Phase Transfer of Nanoparticles across Liquid/Gel Interfaces. Angewandte Chemie - International Edition, 2009, 48, 4953-4956.	7.2	39
45	Water-soluble gold nanoclusters with pH-dependent fluorescence and high colloidal stability over a wide pH range via co-reduction of glutathione and citrate. RSC Advances, 2014, 4, 22651-22659.	1.7	38
46	Fe–Ni Alloy Nanoclusters Anchored on Carbon Aerogels as Highâ€Efficiency Oxygen Electrocatalysts in Rechargeable Zn–Air Batteries. Small, 2021, 17, e2102002.	5.2	38
47	Water-Dispersible Spherically Hollow Clusters of Magnetic Nanoparticles. Chemistry of Materials, 2009, 21, 2442-2451.	3.2	37
48	Controlled synthesis of polyaniline nanostructures with junctions using in situ self-assembly of magnetic nanoparticles. Journal of Materials Chemistry, 2005, 15, 4161.	6.7	36
49	Fabrication of polymeric hollow nanospheres, hollow nanocubes and hollow plates. Nanotechnology, 2006, 17, 1661-1667.	1.3	36
50	Simple Synthesis of Au–Pd Alloy Nanowire Networks as Macroscopic, Flexible Electrocatalysts with Excellent Performance. ACS Applied Materials & Interfaces, 2018, 10, 602-613.	4.0	36
51	Flux method growth of bulk MoS ₂ single crystals and their application as a saturable absorber. CrystEngComm, 2015, 17, 4026-4032.	1.3	35
52	Self-assembled oriented conducting polyaniline nanotubes. Nanotechnology, 2004, 15, 1807-1811.	1.3	34
53	Template-directed synthesis of nitrogen- and sulfur-codoped carbon nanowire aerogels with enhanced electrocatalytic performance for oxygen reduction. Nano Research, 2017, 10, 1888-1895.	5.8	34
54	Synthesis of S-doped AuPbPt alloy nanowire-networks as superior catalysts towards the ORR and HER. Journal of Materials Chemistry A, 2020, 8, 23906-23918.	5.2	32

#	Article	IF	CITATIONS
55	Modulation of Localized Surface Plasmon Resonance of Nanostructured Gold Crystals by Tuning Their Tip Curvature with Assistance of Iodide and Silver(I) Ions. Journal of Physical Chemistry C, 2011, 115, 7887-7895.	1.5	28
56	Effect of Latent Heat in Boiling Water on the Synthesis of Gold Nanoparticles of Different Sizes by using the Turkevich Method. ChemPhysChem, 2015, 16, 447-454.	1.0	28
57	Formation of Hybrid Perovskite Tin Iodide Single Crystals by Topâ€&eeded Solution Growth. Angewandte Chemie, 2016, 128, 3508-3511.	1.6	28
58	Simple synthesis and surface facet-tuning of ultrathin alloy-shells of Au@AuPd nanoparticles <i>via</i> silver-assisted co-reduction onto facet-controlled Au nanoparticles. Journal of Materials Chemistry A, 2018, 6, 7675-7685.	5.2	28
59	Fe ultra-small particles anchored on carbon aerogels to enhance the oxygen reduction reaction in Zn-air batteries. Journal of Materials Chemistry A, 2021, 9, 6861-6871.	5.2	28
60	Empirical structural design of core@shell Au@Ag nanoparticles for SERS applications. Journal of Materials Chemistry C, 2016, 4, 6649-6656.	2.7	27
61	Passively Q-switched mid-infrared laser pulse generation with gold nanospheres as a saturable absorber. Optics Letters, 2018, 43, 1179.	1.7	27
62	Regulating Surface Facets of Metallic Aerogel Electrocatalysts by Size-Dependent Localized Ostwald Ripening. ACS Applied Materials & Interfaces, 2018, 10, 23081-23093.	4.0	26
63	Radiation preparation of nano-powdered styrene-butadiene rubber (SBR) and its toughening effect for polystyrene and high-impact polystyrene. Radiation Physics and Chemistry, 2007, 76, 1732-1735.	1.4	25
64	Rationalized Fabrication of Structure-Tailored Multishelled Hollow Silica Spheres. Chemistry of Materials, 2019, 31, 7470-7477.	3.2	25
65	Compressive Strain in Core–Shell Au–Pd Nanoparticles Introduced by Lateral Confinement of Deformation Twinnings to Enhance the Oxidation Reduction Reaction Performance. ACS Applied Materials & Interfaces, 2019, 11, 46902-46911.	4.0	25
66	Promoting charge transfer in hyperbranched, trisoctahedral-shaped core–shell Au@PdPt nanoparticles by facet-dependent construction of transition layers as high performance electrocatalysts. Journal of Materials Chemistry A, 2017, 5, 18878-18887.	5.2	24
67	Enhanced p-i-n type perovskite solar cells by doping AuAg@AuAg core-shell alloy nanocrystals into PEDOT:PSS layer. Organic Electronics, 2018, 52, 309-316.	1.4	22
68	Fe(<scp>ii</scp>)-Assisted one-pot synthesis of ultra-small core–shell Au–Pt nanoparticles as superior catalysts towards the HER and ORR. Nanoscale, 2020, 12, 20456-20466.	2.8	22
69	Cyclodextrin-assisted synthesis of water-dispersible polyaniline nanofibers by controlling secondary growth. Materials Chemistry and Physics, 2012, 133, 459-464.	2.0	21
70	In situ crystals as templates to fabricate rectangular shaped hollow polyaniline tubes and their application in drug release. Journal of Materials Chemistry, 2011, 21, 2463.	6.7	19
71	Synthesis of Janus Particles <i>via</i> Strain-Driven Microphase Separation and Their Assembly into Nanoscale Vesicles. ACS Nano, 2014, 8, 11206-11213.	7.3	19
72	Large-Area Monolayer Films of Hexagonal Close-Packed Au@Ag Nanoparticles as Substrates for SERS-Based Quantitative Determination. ACS Applied Materials & Interfaces, 2022, 14, 13480-13489.	4.0	19

#	Article	IF	CITATIONS
73	Crown ether derivative assisted growth of oriented polyaniline nanotubes. Nanotechnology, 2006, 17, 3957-3961.	1.3	16
74	Revitalizing spherical Au@Pd nanoparticles with controlled surface-defect density as high performance electrocatalysts. Journal of Materials Chemistry A, 2017, 5, 6992-7000.	5.2	16
75	Realizing enhanced luminescence of silver nanocluster–peptide soft hydrogels by PEI reinforcement. Soft Matter, 2018, 14, 8352-8360.	1.2	16
76	Facet-Dependent Long-Term Stability of Gold Aerogels toward Ethylene Glycol Oxidation Reaction. ACS Applied Materials & Interfaces, 2020, 12, 39033-39042.	4.0	15
77	Simple synthesis of uniformly small gold nanoparticles for sensitivity enhancement in colorimetric detection of Pb ²⁺ by improving nanoparticle reactivity and stability. Journal of Materials Chemistry C, 2018, 6, 637-645.	2.7	12
78	pH-Dependent growth of atomic Pd layers on trisoctahedral gold nanoparticles to realize enhanced performance in electrocatalysis and chemical catalysis. Nanoscale, 2018, 10, 22302-22311.	2.8	12
79	Two-dimensional Au & Ag hybrid plasmonic nanoparticle network: broadband nonlinear optical response and applications for pulsed laser generation. Nanophotonics, 2020, 9, 2537-2548.	2.9	12
80	Transition metal ion-assisted synthesis of monodisperse, quasi-spherical gold nanocrystals via citrate reduction. CrystEngComm, 2014, 16, 5268.	1.3	11
81	Fabrication of Au aerogels with {110}-rich facets by size-dependent surface reconstruction for enzyme-free glucose detection. Journal of Materials Chemistry B, 2019, 7, 7588-7598.	2.9	10
82	Nano-Architecture by Molecular Structure-Directing Agent. Chemistry of Materials, 2008, 20, 2432-2434.	3.2	9
83	Synthesis of large gold nanoparticles with deformation twinnings by one-step seeded growth with Cu(<scp>ii</scp>)-mediated Ostwald ripening for determining nitrile and isonitrile groups. Nanoscale, 2020, 12, 16934-16943.	2.8	9
84	Macroscopical monolayer films of ordered arrays of gold nanoparticles as SERS substrates for <i>in situ</i> quantitative detection in aqueous solutions. Nanoscale, 2021, 13, 14925-14934.	2.8	9
85	Radiation-induced graft polymerization of maleic acid and maleic anhydride onto ultra-fine powdered styrene–butadiene rubber (UFSBR). Radiation Physics and Chemistry, 2007, 76, 1741-1745.	1.4	8
86	Synthesis of composition and size controlled AuAg alloy nanocrystals via Fe ²⁺ -assisted citrate reduction. CrystEngComm, 2016, 18, 7154-7162.	1.3	7
87	S-doped AuPd aerogels as high efficiency catalysts for the oxygen reduction reaction by balancing the ratio between bridging S ₂ ^{2â^'} and apical S ^{2â^'} ligands. Journal of Materials Chemistry A, 2022, 10, 7800-7810.	5.2	5
88	Controlled Synthesis of <1>Y-Junction Polyaniline Nanorods and Nanotubes Using <1>In Situ Self-Assembly of Magnetic Nanoparticles. Journal of Nanoscience and Nanotechnology, 2006, 6, 3950-3954.	0.9	3
89	Oriented Gold Nanoparticle-Polyaniline Nanorods with Nanofibers of Controlled Density on Their Surface. Journal of Nanoscience and Nanotechnology, 2010, 10, 2409-2415.	0.9	3
90	Synthesis of Uniform Gold Nanorods with Large Width to Realize Ultralow SERS Detection. Chemistry - A European Journal, 2021, 27, 7549-7560.	1.7	3

#	Article	IF	CITATIONS
91	Realization of the dehydrogenation pathway of formic acid oxidation by ultra-small core–shell Au–Pt nanoparticles with discrete Pt shells. Materials Advances, 2022, 3, 2786-2792.	2.6	3
92	A detailed study of growth of nanostructured poly(aniline) particles in the light of thermodynamic interaction balance. Physical Chemistry Chemical Physics, 2010, 12, 11905.	1.3	2
93	Shape transformation of gold nanoparticles in aqueous CTAB/CTAC solution to generate high-index facets for electrocatalysis and SERS activity. ChemPhysMater, 2023, 2, 97-113.	1.4	2
94	Preparation of Porous Hollow Polyaniline Microspheres and Study on Their <i>In Vitro</i> Release Behavior. Journal of Nanoscience and Nanotechnology, 2013, 13, 3004-3010.	0.9	1
95	Synthesis of Polyaniline-Coated Carbon Nanotubes and Study on Their pH-Sensitive Conductivity. Journal of Nanoscience and Nanotechnology, 2014, 14, 3087-3094.	0.9	0
96	High Yield Seedless Synthesis of Uniform Silver Nanoparticles with Different Sizes. Journal of Nanoscience and Nanotechnology, 2016, 16, 5824-5828.	0.9	0
97	<i>A Special Section on</i> Nanomaterial for Energy, Environment and Biology. Journal of Nanoscience and Nanotechnology, 2016, 16, 5433-5434.	0.9	0